



大鼠脑出血后内源性神经干细胞迁移和微环境中免疫细胞表型变化规律的关系*

林容旭¹, 樊朝凤¹, 崔文耀¹, 冷静思¹, 贺民¹, 王焱超^{1,2Δ}

1. 四川大学华西医院 神经外科(成都 610041); 2. 四川大学“医学+材料”中心(成都 610044)

【摘要】 目的 研究脑出血(intracerebral hemorrhage, ICH)后内源性神经干细胞(endogenous neural stem cells, eNSCs)及再生微环境的变化规律,观察eNSCs迁移与微环境免疫细胞极化状态变化规律之间的关系,为临床神经修复研究提供研究基础。方法 采用胶原酶注射法造模,在体质量为280~300 g的成年雌性Sprague-Dawley大鼠脑组织注射Ⅶ型胶原酶(2 U)诱导脑出血,为模拟急性期(1周内)、亚急性期(1~3周)及慢性期(>3周)脑出血的时间点,在注射后第3天(3-day post injection, 3 DPI)、10 DPI、20 DPI、30 DPI取脑组织评价造模效果。采用DCX抗体对脑组织切片进行免疫荧光染色,观察不同时间脑组织中eNSCs迁移变化规律;采用CD206抗体、CD86抗体对脑组织切片进行免疫荧光染色,分别观察脑组织促炎型(M1型)免疫细胞和抑炎型(M2型)免疫细胞在脑出血后再生微环境变化规律。结果 在SD大鼠脑组织内注射Ⅶ型胶原酶可成功诱导大鼠自发性脑出血,血肿体积自3 DPI开始逐渐增加,到10 DPI时血肿体积达到最大。此后血肿逐渐吸收,在30 DPI时全部吸收。对脑组织eNSCs变化规律分析显示,在3 DPI时有少量eNSCs被激活但很快便减少,在10 DPI时eNSCs逐渐开始增多,到20 DPI时有大量eNSCs迁移至脑出血部位,而在30 DPI时eNSCs又明显减少($P<0.01$)。对脑组织免疫微环境分析显示,促炎型(M1型)免疫细胞在10、20 DPI时明显增加($P<0.01$),在30 DPI时减少。抑炎型(M2型)免疫细胞在3 DPI时开始逐渐增加,到20 DPI时明显减少($P<0.05$),而在30 DPI时又出现增加。结论 大鼠脑出血后,向脑出血部位迁移的eNSCs先增多后减少,免疫微环境表现出先抑炎、再促炎、最后抑炎的变化规律。炎症对eNSCs迁移可能有刺激作用,但是过强的炎症激活对eNSCs的分化及进一步激活有抑制作用。脑出血后修复及脑保护早期(10 d内)及亚急性期(20 d内)可能是最佳的干预时机。

【关键词】 脑出血 微环境 内源性干细胞 脑组织修复 动物模型

Relationship Between the Migration of Endogenous Neural Stem Cells and the Pattern of Change in Immune Cell Phenotypes in the Microenvironment After Intracerebral Hemorrhage in Rats LIN Rongxu¹, FAN Chaofeng¹, CUI Wenyao¹, LENG Jingsi¹, HE Min¹, WANG Yanchao^{1,2Δ}. 1. Department of Neurosurgery, West China Hospital, Sichuan University, Chengdu 610041, China; 2. Med-X Center of Materials, Sichuan University, Chengdu 610044, China

Δ Corresponding author, E-mail: wangyanchao@wchscu.edu.cn

【Abstract】 **Objective** Intracerebral hemorrhage (ICH), the second most common type of stroke, can cause long-lasting disability in the afflicted patients. The study was conducted to examine the patterns of change in endogenous neural stem cells (eNSCs) and in the regenerative microenvironment after ICH, to observe the relationship between the migration of eNSCs and the pattern of change in the polarization state of immune cells in the microenvironment, and provide a research basis for research on clinical nerve repair. **Methods** The collagenase injection method was used for modeling. The ICH model was induced in adult female Sprague-Dawley (SD) rats by injecting type VII collagenase (2 U) into the brain tissue of rats. All the experimental rats weighed 280-300 g. In order to simulate the ICU at different time points, including the acute phase (within 1 week), subacute phase (1-3 weeks), and the chronic phase (over 3 weeks), brain tissues were harvested at 3 day post injection (3 DPI), 10 DPI, 20 DPI, and 30 DPI to evaluate the modeling effect. Immunofluorescence staining of the brain tissue sections was performed with DCX antibody to observe the pattern of change in the migration of eNSCs in the brain tissue at different time points. Immunofluorescence staining of brain tissue sections was performed with CD206 antibody and CD86 antibody for respective observation of the pattern of change in pro-inflammatory (M1-type) and anti-inflammatory (M2-type) immune cells in the regenerative microenvironment of the brain tissue after ICM. **Results** Spontaneous ICH was successfully induced by injecting type VII collagenase into the brain tissue of SD rats. The volume of the hematoma formed started to gradually increase at 3 DPI and reached its maximum at 10 DPI. After that, the hematoma was gradually absorbed and was completely absorbed by 30 DPI. Analysis of the pattern of changes in eNSCs in the brain tissue showed that a small number of eNSCs were activated at 3 DPI, but

* 国家自然科学基金青年项目(No. 52003177)和四川省科技计划重点研发项目(No. 2022YFS0141)资助

Δ 通信作者, E-mail: wangyanchao@wchscu.edu.cn

出版日期: 2024-05-20

very soon their number started to decrease. By 10 DPI, eNSCs gradually began to increase. A large number of eNSCs migrated to the hemorrhage site at 20 DPI. Then the number of eNSCs decreased significantly at 30 DPI ($P<0.01$). Analysis of the immune microenvironment of the brain tissue showed that pro-inflammatory (M1 type) immune cells increased significantly at 10 and 20 DPI ($P<0.01$) and decreased at 30 DPI. Anti-inflammatory (M2 type) immune cells began to increase gradually at 3 DPI, decreased significantly at 20 DPI ($P<0.05$), and then showed an increase at 30 DPI.

Conclusion After ICH in rats, eNSCs migrating toward the site of ICH first increase and then decrease. The immune microenvironment demonstrates a pattern of change in which inflammation is suppressed at first, then promoted, and finally suppressed again. Inflammation may have a stimulatory effect on the migration of eNSCs, but excessive inflammatory activation has an inhibitory effect on the differentiation and further activation of eNSCs. After ICH, the early stage of repair and protection (10 d) and the subacute phase (20 d) may provide the best opportunities for intervention.

【Key words】 Intracerebral hemorrhage Microenvironment Endogenous neural stem cells Brain repair Animal model

脑出血是神经外科临床常见病、多发病,在脑卒中各亚型中的发病率仅次于缺血性脑卒中,位居第二,我国脑出血患者占有脑卒中患者的18.8%~47.6%^[1]。脑出血后患者多伴有长期神经功能障碍,可引起患者终身残疾,给患者带来严重的经济负担^[2]。随着我国人口老龄化的进展以及高血压等慢性疾病的增加,脑出血的防治显得至关重要。中枢神经组织损伤修复,尤其是脑组织损伤修复,是再生医学亟待解决的重大生物学及医学难题。研究显示,成年哺乳动物中存在一种具有自我更新和分化潜能的内源性神经干细胞(endogenous neural stem cells, eNSCs)^[3-4]。而脑出血可以激活室管膜下区的eNSCs增殖,并迁移至脑出血病灶处^[5]。

最新研究表明,虽然脑出血后eNSCs可迁移至出血部位,但eNSCs无法修复受损脑组织^[6]。这主要归因于脑出血后的细胞毒性物质的释放和炎症通路激活所引起的再生微环境改变,这一过程通常被称为“二次损伤”^[7-8]。“二次损伤”的变化主要以微环境免疫细胞的极化状态变化为主。M1型(促炎型)和M2型(抑炎型)极化是脑出血后免疫细胞的主要极化方式。M1型极化的免疫细胞主要促进炎症的进展,造成组织的进一步损伤;而M2型极化的免疫细胞则缓解炎症进展并促进局部组织的修复^[9]。目前,对于脑出血后内源性修复的研究主要聚焦在对“二次损伤”的干预^[10-11]。然而,对于干预时间的选择高度依赖于eNSCs迁移随时间以及迁移规律的了解。同时,了解再生微环境中免疫细胞极化状态和eNSCs迁移规律之间的关系具有重要意义。目前,多数研究主要集中在eNSCs在损伤后迁移持续的时间及免疫细胞极化状态随时间变化的时间规律^[12-13]。然而,对于出血后不同时间段eNSCs的迁移至损伤部位的变化规律,以及eNSCs迁移与局部微环境免疫细胞极化状态之间关系的研究较少。因此,本研究使用胶原酶法构建大鼠脑出血模型,探索在实验动

物脑出血模型中eNSCs随时间迁移变化规律,并观察eNSCs迁移与微环境免疫细胞极化状态变化规律之间的关系,为脑出血后的治疗和预后提供依据。

1 材料与方 法

1.1 主要试剂和仪器

1.1.1 实验动物、主要试剂

成年雌性Sprague-Dawley大鼠(280~300 g),购自四川大学实验动物中心,生产许可证号:SCXK(川)2018-026,本研究严格遵守四川大学华西医院实验动物伦理委员会的要求(批准号20230227080);异氟烷购自深圳瑞沃德生命科技公司;肝素钠和Ⅶ型胶原酶购自美国Sigma公司;骨蜡和缝合线购自强生(中国)有限公司;体积分数4%多聚甲醛和抗荧光淬灭剂购自上海碧云天生物公司;DCX抗体(Cat# ab153668)、CD206抗体(Cat# ab64693)和Alexa Fluor®488均购自美国Abcam公司;CD86抗体(Cat#PA5-88, 284)购自美国Invitrogen公司。

1.1.2 主要仪器

脑立体定位仪、电动磨钻(深圳瑞沃德生命科技公司);冷冻切片机(Leica, 美国);尼康A1R MP+激光扫描共聚焦显微镜(Nikon, 日本)。

1.2 方 法

1.2.1 脑出血模型构建及取材

采用立体定向仪注射法,在大鼠的运动中枢M1区注射Ⅶ型胶原酶建立大鼠脑出血实验模型。大鼠经1.5%异氟醚吸入麻醉后固定于脑立体定位仪上,头部术区消毒后中线切开头皮,采用立体定位仪精确定位大鼠运动中枢M1区皮层位置。使用电动磨钻形成约3 mm的骨窗。使用微量注射器向M1区(皮质表面下方3 mm)精确注射Ⅶ型胶原酶(2 U),注射后停留10 min后拔出注射器,用骨蜡封闭骨窗后缝合皮肤切口。术后将大鼠置于温度

22~24℃,相对湿度40%~70%的环境中饲养,每日消毒手术区头皮。为模拟(1周内)、亚急性期(1~3周)及慢性期(>3周)脑出血的时间点,实验分别于注射后第3天(3-day post injection, 3 DPI)、10 DPI、20 DPI、30 DPI使用二氧化碳处死动物,立即使用肝素钠(50 U/mL)进行血管内灌注,清除血液;随后用体积分数为4%的多聚甲醛进行血管内缓慢灌注,进行脑组织固定,待固定完成后取出完整脑组织(图1)。

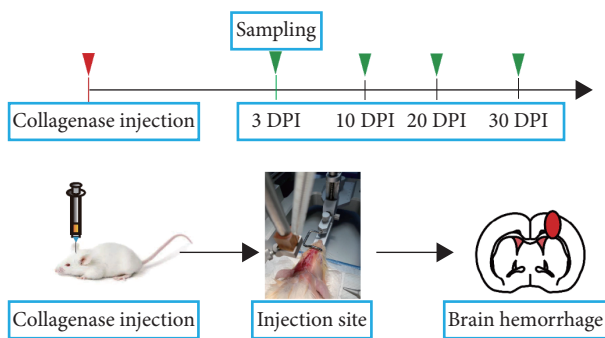


图1 脑出血诱导方法及取材时间

Fig 1 Method of inducing intracerebral hemorrhage and sampling time points

3 DPI: 3-day post injection.

1.2.2 脑缺血模型评价及血肿体积计算方法

将大鼠脑组织进行冰冻切片(厚度2 mm),观察血肿形成及分布情况。使用游标卡尺分别测量血肿的上下径、左右径以及前后径(mm),血肿体积=2×上下径×左右径×前后径/3。

1.2.3 脑组织免疫组织化学法观察eNSCs迁移变化规律

采用脑组织免疫组织化学法分析eNSCs向血肿迁移变化规律。经体积分数为4%的多聚甲醛固定后,使用冷冻切片将脑组织沿轴位切成20 μm切片,用0.3%的Triton X-100溶液中孵育15 min,室温下在封闭缓冲液中封闭40 min;然后将切片与抗DCX抗体(1:200)在4℃孵育过夜;PBS洗涤3次后,将组织与Alexa Fluor®488二抗(1:1000)在37℃孵育1 h后,室温下与DAPI孵育10 min,封片后,尼康A1R MP+激光扫描共聚焦显微镜进行图像采集。图像使用Image J软件(美国)分析荧光分布面积。通过分析出血后不同时间点免疫荧光趋势及荧光分布面积观察eNSCs向血肿迁移的规律。

1.2.4 脑出血后免疫微环境的变化规律

研究采用脑组织免疫组织化学法分析脑出血后免疫微环境的变化规律。脑组织切片制备及处理方法如1.2.3所述。使用抗M1型免疫细胞的抗CD86抗体(1:100)及抗M2型免疫细胞的抗CD206抗体(1:200),

分别标记切片脑组织,4℃孵育过夜;PBS洗涤3次后,将组织与Alexa Fluor®488二抗(1:1000)于37℃孵育1 h后,室温下与DAPI孵育10 min,封片后,尼康A1R MP+激光扫描共聚焦显微镜进行图像采集。使用Image J软件(美国)对于荧光分布面积进行分析。通过观察出血后不同时间点M1型免疫细胞、M2型免疫细胞荧光分布面积变化,分析脑出血后免疫微环境的变化规律。

1.3 统计学方法

定量资料均用 $\bar{x} \pm s$ 表示,每个实验至少重复3次。多组间采用单因素方差分析(ANOVA),两组间比较采用LSD-*t*检验, $P < 0.05$ 为差异有统计学意义。

2 结果

2.1 胶原酶诱导脑出血模型的评价

诱导脑出血后,在预设时间点取大鼠脑组织并进行薄层切片以评价脑出血情况及血肿体积。结果显示,自3 DPI脑组织内部开始出现血肿,10 DPI时血肿体积进一步扩大;而20 DPI时血肿体积较10 DPI时减小,到30 DPI时血肿消失,仅残留脑出血后的创腔,提示脑内出血已被完全吸收(图2,黄色方框)。结果提示,通过注射Ⅶ胶原酶,我们成功构建了大鼠脑出血模型。该模型重复性良好,能够客观反映脑出血发展过程及转归。

2.2 eNSCs向血肿迁移的规律

在本研究中,我们选取血肿与脑组织交界处观察eNSCs的迁移规律,图3中箭头所指方向为血肿所在部位,箭头反方向为远离血肿方向。荧光定量统计选取血肿周围500 μm范围内的荧光信号进行分析。结果表明,从3 DPI开始,血肿周围(图3A,红色箭头所指方向)即出现少量的eNSCs(图3A,绿色荧光标记细胞)。到10 DPI时,可见大量的eNSCs迁移至血肿周围,但是靠近血肿部位的eNSCs较少。到20 DPI时,整个血肿周围出现了大量的eNSCs,提示大量eNSCs迁移至血肿周围。而到30 DPI时,血肿周围的eNSCs明显减少,仅有少量的eNSCs聚集于血肿周围,20 DPI的免疫荧光面积明显大于3、10、30 DPI的免疫荧光面积($P < 0.01$,图3B)。以上结果提示,eNSCs在脑出血后血肿周围呈现先增多后减少的趋势。

2.3 脑出血后免疫微环境的变化规律

为了进一步探索eNSCs在脑出血后向血肿部位迁移规律与微环境变化之间的联系。我们在3、10、20、30 DPI对脑组织中免疫细胞极化状态进行了观察(图4、图5)。我们同样对血肿周围500 μm范围内的荧光信号进行分析。结果显示,在3 DPI时,血肿周围M1(促炎)型的免疫

细胞(图4A, CD86绿色荧光标记)激活逐渐增加, 10 DPI时明显(与3 DPI比较, $P<0.01$), 20 DPI时达到高峰(与3 DPI比较, $P<0.01$; 与10 DPI比较, $P<0.05$), 而在30 DPI明显减少(图4B, 与10 DPI、20 DPI比较, $P<0.01$)。M2(抑

炎)型的免疫细胞(图5A, CD206黄色荧光标记)激活则从3 DPI开始逐渐增加, 10 DPI时达到高峰, 20 DPI时明显减少(与3 DPI、10 DPI、30 DPI相比, $P<0.05$), 到30 DPI时又出现增加(图5B)。

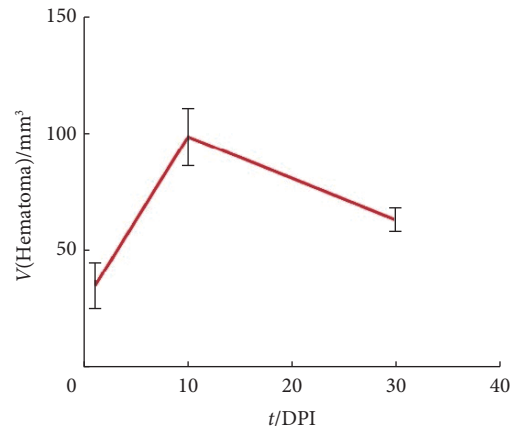
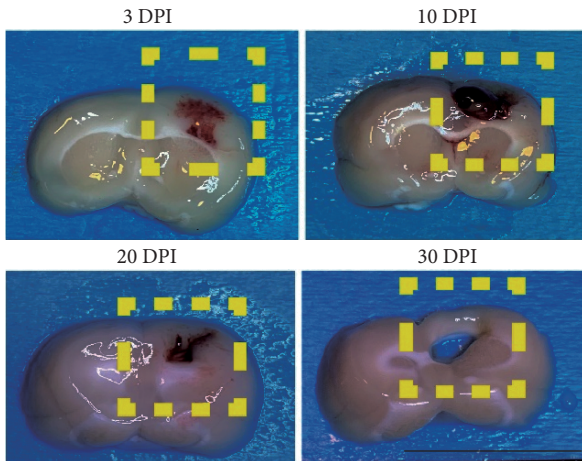


图 2 脑出血诱导大体结果

Fig 2 Gross specimen results of induced intracerebral hemorrhage

Left, Gross section of rat intracerebral hemorrhage. The yellow squares indicate hematoma (scale bar=1 cm). Right, Quantitative analysis of hematoma volume. The data are presented as the $\bar{x} \pm s$ ($n=3$).

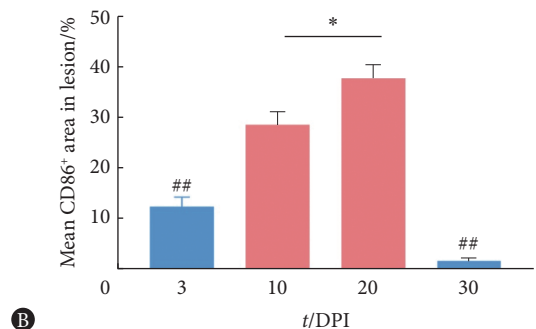
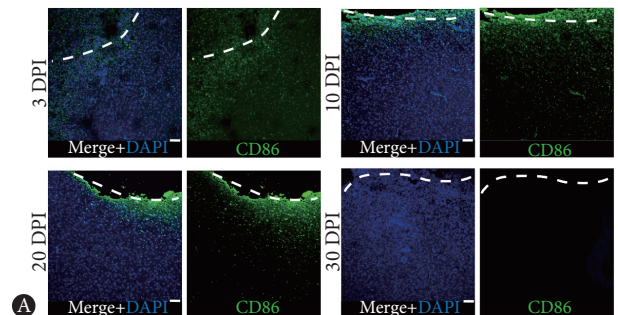
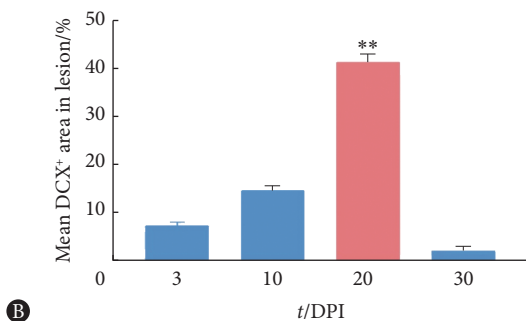
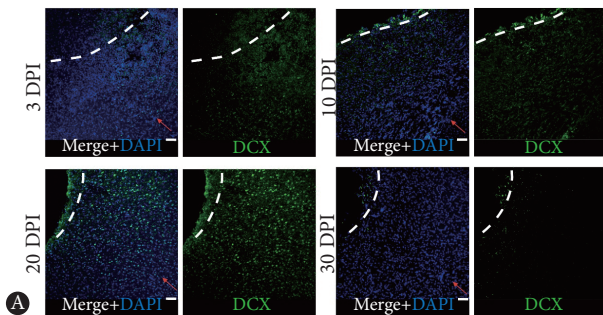


图 3 脑出血后eNSCs迁移至损伤部位的时间变化规律(虚线以上为血肿)

Fig 3 Changes over time in the migration of eNSCs to the site of injury after intracerebral hemorrhage (the section above the dashed line is the hematoma)

A, The migration of endogenous neural stem cells at different time points post brain hemorrhage. The magnified images are located at the bottom on the left. The red arrow indicate the migration direction of eNSCs (scale bar=100 μ m). B, Quantitative analysis of the number of eNSCs ($n=3$). ** $P<0.01$, vs. 3 DPI, 10 DPI, 30 DPI.

图 4 脑出血后M1型免疫细胞随时间变化的规律(虚线以上为血肿)

Fig 4 Pattern of changes in the activation state of M1-like immune cells after intracerebral hemorrhage (the section above the dashed line is the hematoma)

A, Polarization of M1-like immune cells at each time point post brain hemorrhage. M1-like immune cells showed significant activation at 10 and 20 DPI post hemorrhage. The magnified images are located at the bottom on the left (scale bar=100 μ m). B, Quantitative analysis of the number of M1-like immune cells ($n=3$). * $P<0.05$. ** $P<0.01$, vs. 10 DPI, 20 DPI.

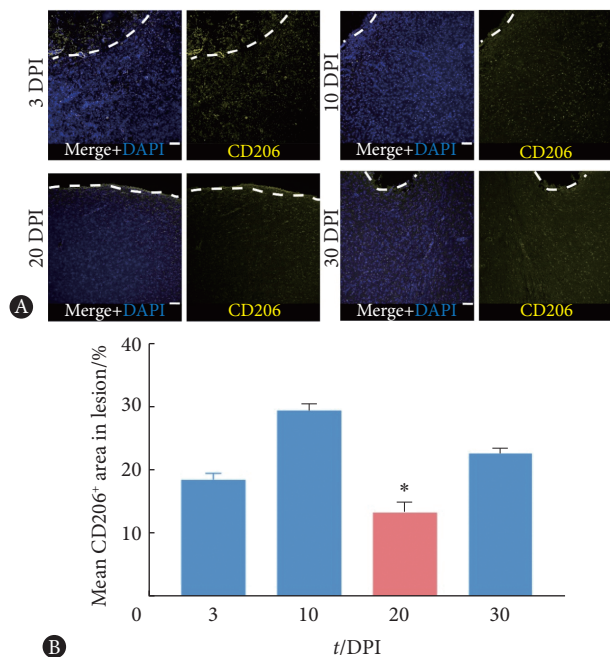


图5 脑出血后M2型免疫细胞随时间变化的规律(虚线以上为血肿)
Fig 5 Pattern of changes in the activation state of M2-like immune cells after intracerebral hemorrhage (the section above the dashed line is the hematoma)

A, The polarization of M2-like immune cells at different time points post brain hemorrhage. M2-like immune cells showed significant activation at 10 DPI post hemorrhage. The number of M2-like immune cells dropped at 20 DPI post hemorrhage and slightly increased at 30 DPI post hemorrhage. Magnified images are located at the bottom on the left (scale bar=100 μ m). B, Quantitative analysis of the number of M2-like immune cells ($n=3$). * $P<0.05$, vs. 3 DPI, 10 DPI, 30 DPI.

3 讨论

脑出血后内源性脑组织修复是目前再生医学、神经外科学的研究热点^[14]。如何促进迁移至损伤局部的eNSCs分化为神经元并重建脑组织,是脑修复的核心问题之一^[15]。胶原酶诱导的脑出血模型是目前脑出血动物模型主要构建方式之一^[16]。胶原酶诱导的脑出血模型在脑出血损伤的范围、部位以及恢复情况等方面都有显著差异^[17]。通常认为胶原酶诱导的脑出血模型损伤范围更大,且由于胶原酶对于细胞外基质的破坏,其与人类脑出血损伤的临床表现更为接近^[18]。因此,本研究利用VII型胶原酶诱导脑出血,该方法能够模拟人体脑出血并破坏细胞外基质成分,最大程度还原人类脑出血情况。同时,立体定向注射法能够精确定位于特定脑区,使用微量注射器便于操作,重复性较好,能够稳定诱导脑出血,以利于脑出血后eNSCs迁移及微环境变化的评价。

脑出血后的eNSCs迁移受到许多因素的影响,如细胞外基质成分,细胞因子浓度梯度,局部炎症细胞极化情况

等^[13,19]。为了更好地进行脑组织修复,eNSCs迁移至脑出血部位数量最多时进行干预无疑是最佳的干预时机^[20]。为此,本研究对于大鼠胶原酶诱导的脑出血后脑组织中eNSCs迁移情况进行了分析。同时由于“二次损伤”主要是受到再生微环境中免疫细胞的影响,因此本研究观察了脑出血后脑组织中免疫细胞的激活状态。

结果显示,在3DPI时,脑出血部位出现少量的eNSCs,同时M1及M2型免疫细胞激活均有明显的增加,提示此时炎症及eNSCs的迁移均逐渐开始活跃。到10 DPI时,eNSCs、M1及M2型免疫细胞激活均处于持续上升阶段,说明虽然能够迁移至出血部位的eNSCs逐渐上升,但此时免疫细胞尤其是M1型免疫细胞激活也逐渐增加。M1型免疫细胞的作用主要是促进局部炎症及分泌大量炎症因子,提示在内源性修复增加的同时,“二次损伤”逐渐也在加重。在20 DPI时,迁移至脑出血部位的eNSCs数目达到顶峰,同时M1型免疫细胞激活也达到最多。相反的M2型免疫细胞激活却降至最低,提示此时的炎症反应最重,也说明“二次损伤”在脑出血后的进展趋势与eNSCs迁移的趋势相同,提示炎症对eNSCs迁移可能有刺激作用,但是过强的炎症激活对eNSCs的分化及进一步激活有抑制作用。因此在30 DPI时eNSCs数量下降,且通过大体标本发现,迁移至脑出血部位的eNSCs无法填补脑出血的创腔。最终,在30 DPI时M1型免疫细胞激活下降,M2型免疫细胞激活上升,提示此时炎症反应已趋于平静。然而,由于M1型免疫细胞的过度激活抑制了eNSCs的分化和持续迁移,导致内源性的脑修复无法实现。以上结果证实了“二次损伤”是影响脑内源性修复效果的主要因素的观点^[21]。

综上所述,本研究利用大鼠脑出血模型对脑出血后脑组织中eNSCs迁移变化规律和免疫微环境进行了分析,脑出血后修复及脑保护早期(10 d内)及亚急性期(20 d内)可能是最佳的干预时机。本研究的结果可为脑出血后神经修复的基础研究和临床应用提供研究基础。

* * *

作者贡献声明 林容旭负责正式分析、调查研究、可视化和初稿写作,樊朝凤和崔文耀负责研究项目管理、提供资源和监督指导,冷静思负责验证、可视化和初稿写作,贺民负责研究项目管理、提供资源和监督指导,王焱超负责论文构思、数据审编、正式分析、经费获取、调查研究、研究方法、研究项目管理、提供资源、验证、可视化和审读与编辑写作。所有作者已经同意将文章提交给本刊,且对将要发表的版本进行最终定稿,并同意对工作的所有方面负责。

Author Contribution LIN Rongxu is responsible for formal analysis, investigation, visualization, and writing--original draft. FAN Chaofeng and CUI Wenyao are responsible for project administration, resources, and supervision. LENG Jingsi is responsible for validation, visualization, and writing--original draft. HE Min is responsible for project administration,

resources, and supervision. WANG Yanchao is responsible for conceptualization, data curation, formal analysis, funding acquisition, investigation, methodology, project administration, resources, validation, visualization, and writing--review and editing. All authors consented to the submission of the article to the Journal. All authors approved the final version to be published and agreed to take responsibility for all aspects of the work.

利益冲突 所有作者均声明不存在利益冲突

Declaration of Conflicting Interests All authors declare no competing interests.

参 考 文 献

- [1] 中华医学会神经病学分会, 中华医学会神经病学分会脑血管病学组. 中国脑出血诊治指南(2014). 中华神经科杂志, 2015, 48(6): 435-444. doi: 10.3760/cma.j.issn.1006-7876.2015.06.002.
Chinese Society of Neurology, Chinese Society of Neurology, Chinese Society of Cerebrovascular Disease. Chinese guidelines for the diagnosis and treatment of cerebral hemorrhage (2014). Chin J Neuro, 2015, 48(6): 435-444. doi: 10.3760/cma.j.issn.1006-7876.2015.06.002.
- [2] FELDMANN E, GROTTA J, KASE C, *et al.* Guidelines for the management of spontaneous intracerebral hemorrhage. Stroke, 2015, 46(7): 2032-2060. doi: 10.1161/STR.0000000000000069.
- [3] TANG T, LI X Q, WU H, *et al.* Activation of endogenous neural stem cells in experimental intracerebral hemorrhagic rat brains. Chin Med J (Engl), 2004, 117(9): 1342-1347. doi: 10.1370/afm.226.
- [4] LI W, HUANG X, YU W, *et al.* Activation of functional somatic stem cells promotes endogenous tissue regeneration. J Dent Res, 2022, 101(7): 802-811. doi: 10.1177/00220345211070222.
- [5] YAN Y P, LANG B T, VEMUGANTI R, *et al.* Persistent migration of neuroblasts from the subventricular zone to the injured striatum mediated by osteopontin following intracerebral hemorrhage. J Neurochem, 2010, 109(6): 1624-1635. doi: 10.1111/j.1471-4159.2009.06059.x.
- [6] KEEP R F, HUA Y, XI G. Intracerebral haemorrhage: mechanisms of injury and therapeutic targets. Lancet Neurol, 2012(8): 11. doi: 10.1016/S1474-4422(12)70104-7.
- [7] ZHOU Y, WANG Y, WANG J, *et al.* Inflammation in intracerebral hemorrhage: from mechanisms to clinical translation. Prog Neurobiol, 2014, 115: 25-44. doi: 10.1016/j.pneurobio.2013.11.003.
- [8] WANG J, DORÉ S. Inflammation after intracerebral hemorrhage. J Cereb Blood Flow Metab, 2007, 27(5): 894-908. doi: 10.1038/sj.jcbfm.9600403.
- [9] ALSBROOK D L, Di NAPOLI M, BHATIA K, *et al.* Neuroinflammation in acute ischemic and hemorrhagic stroke. Curr Neurol Neurosci Rep, 2023, 23(8): 407-431. doi: 10.1007/s11910-023-01282-2.
- [10] REN H, HAN R, CHEN X, *et al.* Potential therapeutic targets for intracerebral hemorrhage-associated inflammation: an update. J Cereb Blood Flow Metab, 2020, 40(9): 1752-1768. doi: 10.1177/0271678X2092355.
- [11] LIN J, XU Y, GUO P, *et al.* CCL5/CCR5-mediated peripheral inflammation exacerbates blood-brain barrier disruption after intracerebral hemorrhage in mice. J Transl Med, 2023, 21(1): 196. doi: 10.1186/s12967-023-04044-3.
- [12] MATSUMOTO S, TANAKA J, YANO H, *et al.* CD200+ and CD200- macrophages accumulated in ischemic lesions of rat brain: the two populations cannot be classified as either M1 or M2 macrophages. J Neuroimmunol, 2015, 282: 7-20. doi: 10.1016/j.jneuroim.2015.03.013.
- [13] YIN D, WANG C, QI Y, *et al.* Neural precursor cell delivery induces acute post-ischemic cerebroprotection, but fails to promote long-term stroke recovery in hyperlipidemic mice due to mechanisms that include pro-inflammatory responses associated with brain hemorrhages. J Neuroinflammation, 2023, 20(1): 210. doi: 10.1186/s12974-023-02894-8.
- [14] ZIAI W C, CARHUAPOMA J R. Intracerebral hemorrhage. Continuum (Minneapolis Minn), 2018, 24(6): 1603-1622. doi: 10.1212/CON.0000000000000672.
- [15] MAGID-BERNSTEIN J, GIRARD R, POLSTER S, *et al.* Cerebral hemorrhage: pathophysiology, treatment, and future directions. Circ Res, 2022, 130(8): 1204-1229. doi: 10.1161/CIRCRESAHA.121.319949.
- [16] LEI B, SHENG H, WANG H, *et al.* Intrastratial injection of autologous blood or clostridial collagenase as murine models of intracerebral hemorrhage. J Vis Exp, 2014(89): 51439. doi: 10.3791/51439.
- [17] THANGAMEERAN S I M, PANG C Y, LEE C H, *et al.* Experimental animal models and evaluation techniques in intracerebral hemorrhage. Tzu Chi Med J, 2022, 35(1): 1-10. doi: 10.4103/tcmj.tcmj_119_22.
- [18] MACLELLAN C L, SILASI G, POON C C, *et al.* Intracerebral hemorrhage models in rat: comparing collagenase to blood infusion. J Cereb Blood Flow Metab, 2008, 28(3): 516-525. doi: 10.1038/sj.jcbfm.9600548.
- [19] JIAO Y, PALMGREN B, NOVOZHILOVA E, *et al.* BDNF increases survival and neuronal differentiation of human neural precursor cells cotransplanted with a nanofiber gel to the auditory nerve in a rat model of neuronal damage. Biomed Res Int, 2014, 2014: 356415. doi: 10.1155/2014/356415.
- [20] LIM T C, MANDEVILLE E, WENG D, *et al.* Hydrogel-based therapy for brain repair after intracerebral hemorrhage. Transl Stroke Res, 2020, 11(3): 412-417. doi: 10.1007/s12975-019-00721-y.
- [21] ZHU H, WANG Z, YU J, *et al.* Role and mechanisms of cytokines in the secondary brain injury after intracerebral hemorrhage. Prog Neurobiol, 2019, 178: 101610. doi: 10.1016/j.pneurobio.2019.03.003.

(2024-01-17收稿, 2024-05-09修回)

编辑 何学令



开放获取 本文使用遵循知识共享署名—非商业性使用 4.0国际许可协议(CC BY-NC 4.0), 详细信息请访问

<https://creativecommons.org/licenses/by/4.0/>。

OPEN ACCESS This article is licensed for use under Creative Commons Attribution-NonCommercial 4.0 International license (CC BY-NC 4.0). For more information, visit <https://creativecommons.org/licenses/by/4.0/>.

© 2024 《四川大学学报(医学版)》编辑部 版权所有

Editorial Office of Journal of Sichuan University (Medical Science)